

Effects of Dzyaloshinsky-Moriya Interaction on magnetism in Nanodisks

Zhaosen Liu^{a*}, Hou Ian^b

^a*Department of Applied Physics, Nanjing University of Information Science and Technology, Nanjing 210044, China*

^b*Institute of Applied Physics and Materials Engineering, FST, University of Macau, Macau*

Abstract

We give a theoretical study on the magnetic properties of monolayer nanodisks with both Heisenberg exchange and Dzyaloshinsky-Moriya (DM) interactions. In particular, we survey the magnetic effects caused by anisotropy, external magnetic field, and disk size when DM interaction is present by means of a new quantum simulation method based on mean-field theory. This computational approach finds that uniaxial anisotropy and transverse magnetic field enhances the net magnetization as well as increases the transition temperature of the vortex phase while preserving the chiralities of the nanodisks. Whereas, when the strength of DM interaction is sufficiently strong for a given disk size, magnetic domains appear within the circularly bounded region, which vanish and gives in to a single vortex when a transverse magnetic field is applied. The latter confirms the magnetic skyrmions induced by the magnetic field as observed in the experiments.

PACS numbers: 75.40.Mg, 75.10.Jm

* Email: liuzhsnj@yahoo.com

I. INTRODUCTION

Dzyaloshinsky-Moriya (DM) interaction [1, 2], which arises from the spin-orbit scattering of electrons in an inversely asymmetric crystal field, exists in systems with broken inversion symmetry, such as the metallic alloys with B20 structure [3–7] and the surface or interface of magnetic multi-layers [8, 9]. This interaction is able to induce chiral spin structures, such as skyrmions [10], and other exotic properties, providing the basis for developing new spintronic devices. For instance, in the confined structures such as magnetic nanodisks and nanostripes, DM interaction can produce stable out-of-plane magnetizations as well as in-plane left-handed and right-handed magnetic vortices [11–14].

These exotic magnetic structures have recently been experimentally observed. For examples, Heinze et al. observed a spontaneous atomic-scale magnetic ground-state skyrmion lattice in a monolayer Fe film at a temperature about 11 K [8]; Yu et al. have obtained a skyrmion crystal near room-temperature in FeGe by applying a strong magnetic field [4]. The latter shows the low-temperature constrain [16] which presents for most skyrmions in helimagnets produced by external magnetic fields [3, 6, 15] can be overcome.

In the present work, we use a self-consistent approach (SCA) developed in recent years [17–20] to investigate the special magnetic properties of monolayer nanodisks induced by DM interactions, where the co-existence of Heisenberg exchange and uniaxial anisotropy are assumed. The effectiveness of the approach has been verified on a nanowire consisting of ferromagnetically coupled 3D ions [18] and a $\text{DyNi}_2\text{B}_2\text{C}$ nanoball [20]. The algorithm for this approach, which we brief in Sec. II, is based on the principle of the least free energy. That is, while the algorithm approaches the eventual equilibrium state, the magnetic moments of the system are rotated and their magnitudes adjusted by the local effective field to minimize the system energy spontaneously.

Here, simulations using the SCA algorithm are performed on nanodisks with different sizes and DM interaction strengths and under different scenarios. We start with the simplest case in Sec. III.A, where the lattice is considered isotropic and study the effect of anisotropy in Sec. III.B. The case when both anisotropy and external magnetic field are taken in consideration is discussed in Sec. III.C. We find that a single right-handed (left-handed) magnetic vortex is generated in the disk plane by a $D > 0$ ($D < 0$) DM interaction strength when the disk size is sufficient small (10 times the lattice constant). In addition, an external magnetic

field normal to the disk plane was able to preserve the vortex structure above the transition temperature at $T_M \approx 2.92$ K, making the vortex still observable at 5 K.

The considerations above assume a relatively weak DM interaction where the chiralities of eddy structures are preserved. In Sec. III.E and Sec. III.F, we further increase the interaction strength while simultaneously increase the disk size to a few times the DM length in diameter. We find that multiple magnetic vortices, separated by strips, were formed. The sizes of these magnetic domains agree well with the present theory. In addition, the effect of DM interaction can be cancelled by an external magnetic field normal to the disk, letting the multiple domains merge to a single in-plane vortex. This finding concides with the experimental observations [3, 4, 6, 15].

II. SELF-CONSISTENT APPROACH

The nanosystems we investigated in this work can be described with a Hamiltonian [21]

$$\mathcal{H} = -\frac{1}{2} \left[\sum_{i,j \neq i} \mathcal{J}_{ij} \vec{S}_i \cdot \vec{S}_j - \sum_{i,j \neq i} D_{ij} \vec{r}_{ij} \cdot (\vec{S}_i \times \vec{S}_j) \right] - K_A \sum_i (\vec{S}_i \cdot \hat{n})^2 - \mu_B g_S \vec{B} \cdot \sum_i \vec{S}_i, \quad (1)$$

where the first and second terms represent the Heisenberg exchange and DM interactions with strength of \mathcal{J}_{ij} and D_{ij} between each pair of neighboring spins situated at the i -th and j -th site, respectively, the third term denotes the uniaxial anisotropy along the \hat{n} direction, and the last term is the Zeeman energy of the system within the applied magnetic field \vec{B} . For simplicity, we consider here a few round monolayer nanodisks consisting of $S = 1$ spins, which interact only with their nearest neighbors with uniform strength, that is, $\mathcal{J}_{ij} = \mathcal{J}$ and $D_{ij} = D$ over each disk which is assumed to be in the xy -plane, and the anisotropy is perpendicular to the disk plane, i. e. along the z -axis. In the above Hamiltonian, the spins are quantum operators instead of the classical vectors. Since $S = 1$, the matrices of the three spin components are given by

$$S_x = \frac{1}{2} \begin{pmatrix} 0 & \sqrt{2} & 0 \\ \sqrt{2} & 0 & \sqrt{2} \\ 0 & \sqrt{2} & 0 \end{pmatrix}, \quad S_y = \frac{1}{2i} \begin{pmatrix} 0 & \sqrt{2} & 0 \\ -\sqrt{2} & 0 & -\sqrt{2} \\ 0 & \sqrt{2} & 0 \end{pmatrix}, \quad S_z = \begin{pmatrix} 1 & 0 & 0 \\ 0 & 0 & 0 \\ 0 & 0 & -1 \end{pmatrix}, \quad (2)$$

respectively. And according to quantum theory, the thermal average of any physical quantity A must be evaluated with

$$\langle A \rangle = \frac{\sum_n \langle \varphi_n | \hat{A} \exp(-\varepsilon_n/k_B T) | \varphi_n \rangle}{\sum_n \exp(-\varepsilon_n/k_B T)}, \quad (3)$$

where ε_n and φ_n are the eigenenergy and eigenfunction, respectively, of the related Hamiltonian, for instance, of the considered spin.

All of our recent simulations employing the SCA approach were started from a random magnetic configuration and a temperature above the magnetic transition, then carried out stepwise down to very low temperatures with a temperature step $\Delta T < 0$. This point is *crucial*, since we believe that at high temperatures the interactions among the spins with small magnitudes are considerably weak, the thermal interaction is strong enough to help the spins overcome the energy barriers, so that the code can avoid being trapped in local energy minima, and finally converge down to the equilibrium state of the system with globally least total (free) energy. Obviously, to ensure thermal energy of the spins sufficiently strong at all subsequent temperatures, $|\Delta T|$ cannot be too large. At any temperature T , if the difference $|\langle \vec{S}_i' \rangle - \langle \vec{S}_i \rangle|$ between two successive iterations for every spin is less than a very small given value τ_0 , convergency is considered to be reached.

III. CALCULATED RESULTS

A. Magnetic Properties of a Nanodisk Without Anisotropy

In order to visualize the calculated spin configurations clearly, we first conducted simulations with the SCA approach for a very tiny round monolayer nanodisk, whose radius $R = 10a$, where a is the side length of the square crystal unit cell. Other parameters were assigned to $\mathcal{J}/k_B = 1$ K, $D/k_B = \pm 0.1$ K, and $\Delta T = -0.02$ K, respectively.

For comparison, the influences of both uniaxial anisotropy and the external magnetic field was neglected in simulations at the beginning. Figure 1 displays our calculated spontaneous thermally averaged $\langle S_z \rangle$, $\langle S_x \rangle$ and $\langle S_y \rangle$ for the round nanodisk with the parameters given below the figures. The on-plane DM interaction has indeed induced out-plane magnetic moments [11, 12], which are stronger than the on-plane components in the magnetic phase as displayed in the two sub-figures. As temperature rises, the three components decay

monotonously until the transition temperature $T_M \approx 2.66$ K, and the saturated value of $\langle S_z \rangle$ at very low temperatures is much less than the maximum value $S = 1$.

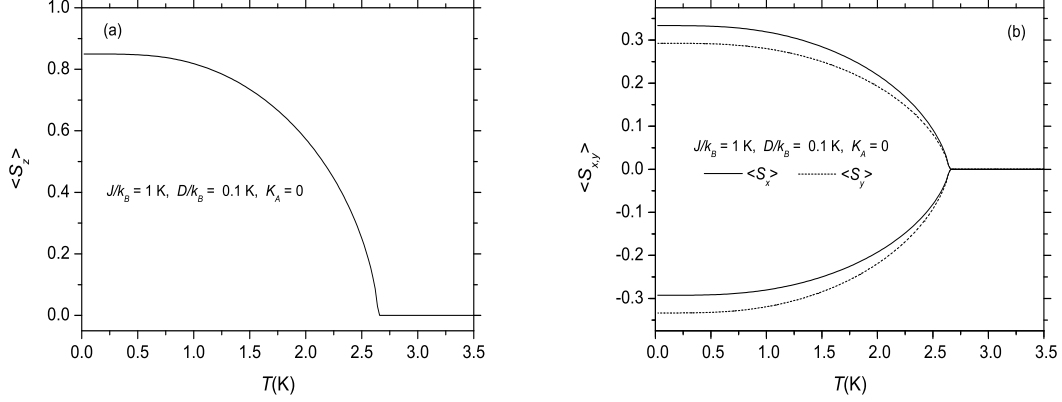


Figure 1. Calculated spontaneous (a) $\langle S_z \rangle$, (b) $\langle S_x \rangle$ and $\langle S_y \rangle$ for the monolayer nanodisk. The used parameters are $R = 10a$, $\mathcal{J}/k_B = 1$ K, and $D/k_B = 0.1$ K, respectively.

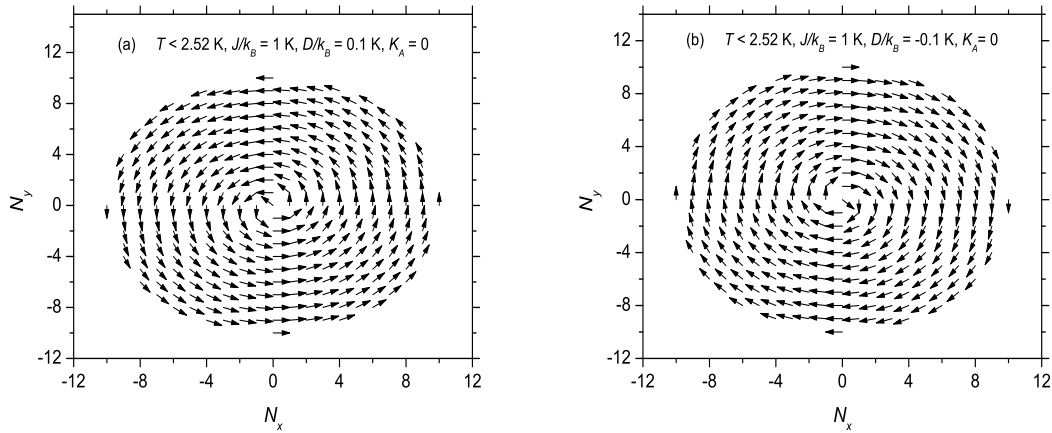


Figure 2. Calculated spin configurations projected onto the xy -plane as (a) $D/k_B = 0.1$ K, and (b) $D/k_B = -0.1$ K in the absence of external magnetic field. Other used parameters are $R = 10a$, $\mathcal{J}/k_B = 1$ K, $K_A/k_B = 0$ K, respectively.

Due to the DM interaction, magnetic vortices are formed on the nanodisks as depicted in Figure 2, they were obtained with D/k_B assigned to ± 0.1 K respectively, but other parameters remained the same as before. In the case of $D/k_B = 0.1$ K, the directions of $\langle S_z \rangle$

and the magnetic vortex in the xy -plane meet the right-hand spiral rule. But when $D/k_B = -0.1$ K, the chirality of the vortex, as displayed in Figure 2(b), is reversed [9]. However, the calculated $\langle S_z \rangle$ curve is now still exactly identical to that obtained with $D/k_B = 0.1$ as plotted in Figure 1(a).

B. Effects of Uniaxial Anisotropy

By taking account of a strong uniaxial anisotropy of $K_A/k_B = 1$ K normal to the disk plane, we performed further simulations. As displayed in Figure 3(a), the transition temperature is now increased to $T_M \approx 2.92$ K, and $\langle S_z \rangle$ becomes almost saturated at very low temperatures. Therefore, $\langle S_z \rangle$ has been considerably enhanced by the uniaxial anisotropy along the same direction. But for the same sake, as shown in Figure 3(b), $\langle S_x \rangle$ and $\langle S_y \rangle$ have been considerably reduced by the anisotropy, and their shapes also changed a lot. On

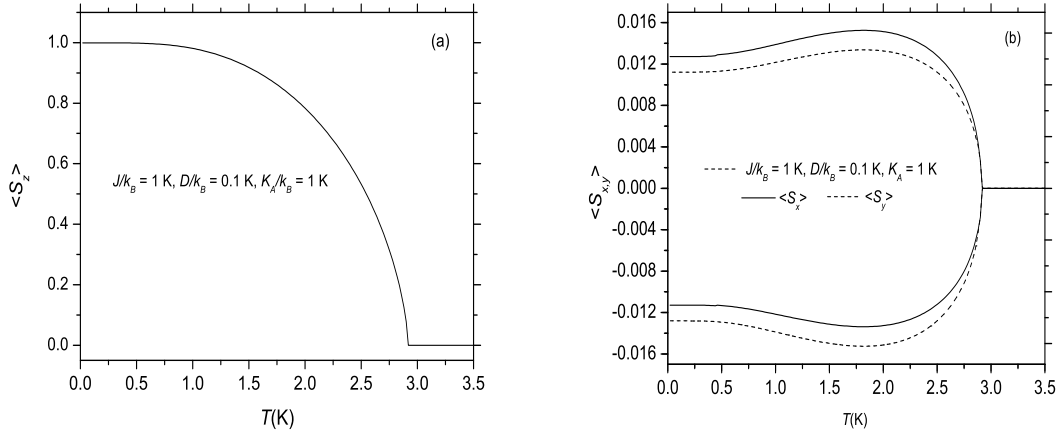


Figure 3. Calculated spontaneous (a) $\langle S_z \rangle$, (b) $\langle S_x \rangle$ and $\langle S_y \rangle$ for the monolayer nanodisk.

Here $R = 10a$, $\mathcal{J}/k_B = 1$ K, $D/k_B = 0.1$ K, and $K_A/k_B = 1$ K, respectively.

the other hand, when $D/k_B = -0.1$ K but other parameters are unchanged, we can still get very similar three components: the $\langle S_z \rangle$ curve remains same, but $\langle S_x \rangle$ and $\langle S_y \rangle$ curves just exchange their positions. In this case, we also obtained almost same magnetic structures as those shown in Figure 2. To short the text, these results are not plotted here. Once again, when $D/k_B = 0.1$ K, the directions of $\langle S_z \rangle$ and the magnetic vortex satisfies the right-hand screw rule; but while $D/k_B = -0.1$ K, the chirality of the vortex is reversed [9]. As $T =$

0.28 K we observed in the both cases that the vectors at the lattice center disappeared. This fact means that, at very low temperatures, the spin at the center has been rotated by the uniaxial anisotropy completely to the direction normal to the disk.

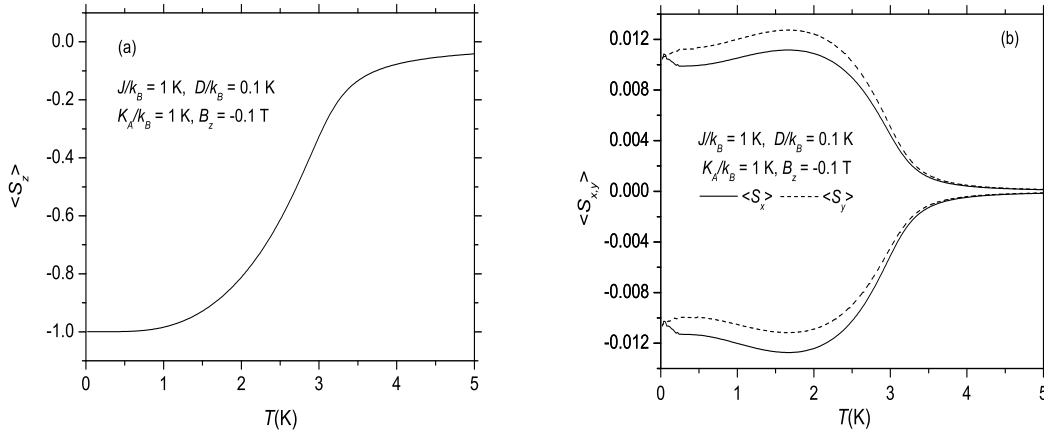


Figure 4. Calculated (a) $\langle S_z \rangle$, (b) $\langle S_x \rangle$ and $\langle S_y \rangle$ for the monolayer nanodisk in a magnetic field of 0.1 Tesla applied antiparallel to the z axis. Other parameters are $R = 10a$, $D/k_B = 0.1$ K, $J/k_B = 1$ K, and $K_A/k_B = 1$ K, respectively.

C. Effects of External Magnetic Field

Later on, a magnetic field antiparallel to the direction of the spontaneous $\langle S_z \rangle$ was considered to do simulations. As displayed in Figure 4, the spontaneous $\langle S_z \rangle$ has been rotated by the applied magnetic field for 180° to its direction. And no matter $D/k_B = 0.1$ or -0.1 K, we obtained the exactly same $\langle S_z \rangle$, $\langle S_x \rangle$ and $\langle S_y \rangle$ curves, the only difference was that as D changed the sign the two transversal components exchanged their positions. The external magnetic field has considerably modified the shapes of the three curves especially in the region around the transition temperature, and strongly enhanced the z -components of the magnetization, so that it persists to much higher temperatures. As depicted in Figure 5, the direction of the magnetic vortex in the xy -plane, which is stable below $T = 4$ K and can still be observed at $T = 5$ K, has also been reversed by the applied magnetic field, however their chiralities are well conserved.

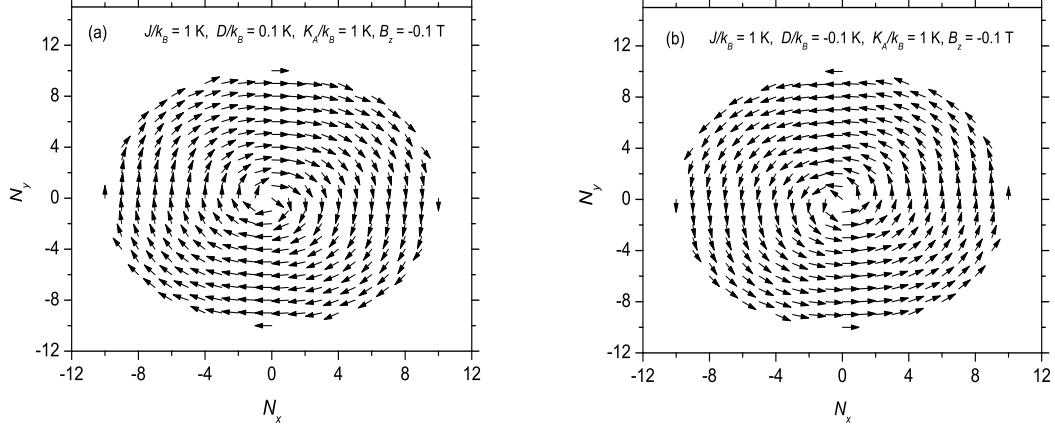


Figure 5. Calculated spin configurations projected onto the xy -plane within an external magnetic field of 0.1 Tesla applied antiparallel to the z direction, as (a) $D/k_B = 0.1$ K, and (b) $D/k_B = -0.1$ K. Other used parameters are $R = 10a$, $\mathcal{J}/k_B = 1$ K, and $K_A/k_B = 1$ K, respectively.

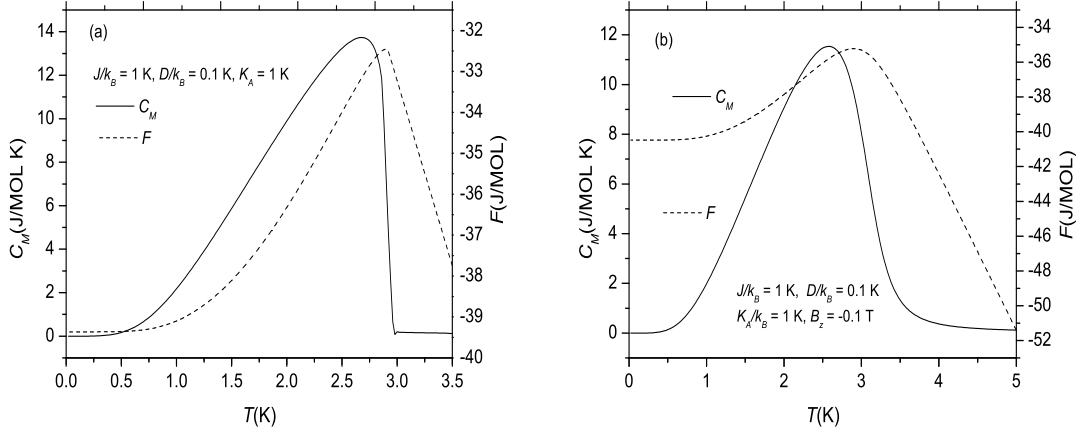


Figure 6. Calculated specific heats and free energies per mole of spins when (a) no external magnetic is applied, and (b) an external magnetic field of 0.1 Tesla is applied antiparallel to the z axis. Other used parameters are $R = 10a$, $\mathcal{J}/k_B = 1$ K, and $K_A/k_B = 1$ K, respectively.

D. Thermodynamic Properties of the Nanodisk

The total free energy F , total energy E , entropy S_M and specific heat C_M of these canonical systems can be evaluated with

$$F = -k_B T \log Z_N, \quad E = -\frac{\partial}{\partial \beta} \log Z_N, \\ S_M = \frac{E}{T} + k_B \log Z_N, \quad C_M = T \left(\frac{\partial S_M}{\partial T} \right)_B, \quad (4)$$

successively, where $\beta = 1/(k_B T)$ and Z_N is the partition function of the whole system. The first three quantities can be calculated during the simulation, but C_M must be computed by using the last formula after the simulation for the whole temperature range has been completed. To shorten the text, only the free energies and specific heats calculated with the SCA approach, both in the absence and presence of external magnetic field exerted antiparallel to the spontaneous $\langle S_z \rangle$, are plotted in Figure 6 for comparison. The parameters used in the simulation are given below the figure. The magnetic behaviors of the nanodisk have been considerably modified by the applied magnetic field, so that the curves near the transition temperature changes smoothly as displayed in Figure 6(b). The peak in each C_M curve is the evidence of phase transition within the narrow temperature interval.

E. Effects of DM Interaction Strength and External Magnetic Field

To deal with the systems with magnetically eddy structures, DM length has been introduced and defined as $\zeta = \mathcal{J}/D$, which is related to the size of self-organized structures [22]. So, as the size of the disk is larger than ζ in the unit of lattice parameter a , more magnetic domains, such as strips and vortices, will be formed.

By increasing the DM Interaction to $D/k_B = 0.3$ K and assuming that no external magnetic field is applied, simulations were then done for the nanodisk. The calculated $\langle S_z \rangle$, $\langle S_x \rangle$ and $\langle S_y \rangle$ are plotted in Figure 7. Now $\zeta = \mathcal{J}/D \approx 3.333$, and $R > \zeta$, so it is expected more self-organized structures will appear. The sudden changes of $\langle S_z \rangle$ and $\langle S_x \rangle$ around 1.3 K indicate that a phase transition occurs nearby. Indeed, above 1.3 K, the magnetic vortex, as shown in Figure 8(a), can still be formed around the disk center. However, below that temperature, a magnetic strip appears between the two magnetic vortices, as displayed in Figure 8(b), whose upper and lower parts are excellently symmetric about the horizontal

line $N_y = 0$.

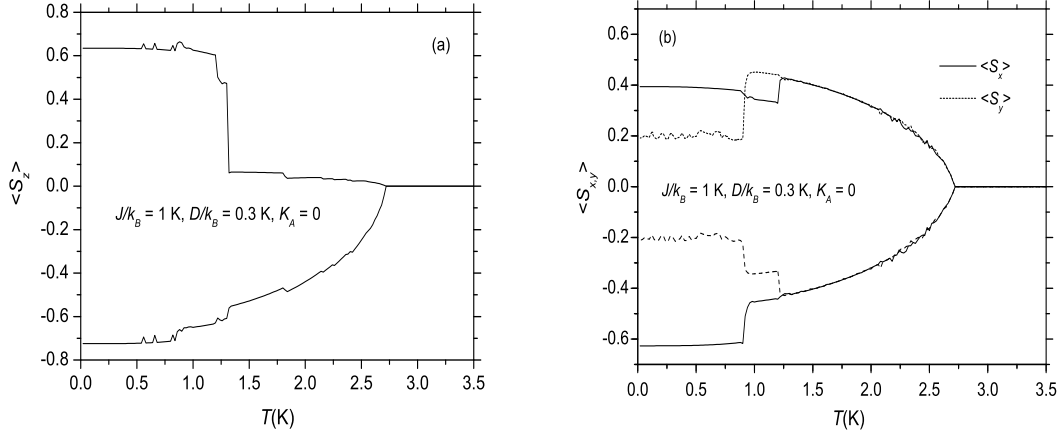


Figure 7. Calculated spontaneous (a) $\langle S_z \rangle$, (b) $\langle S_x \rangle$ and $\langle S_y \rangle$ for the monolayer nanodisk with $D/k_B = 0.3$ K. Other parameters are $R = 10a$, $\mathcal{J}/k_B = 1$ K, and $K_A/k_B = 0$ K.

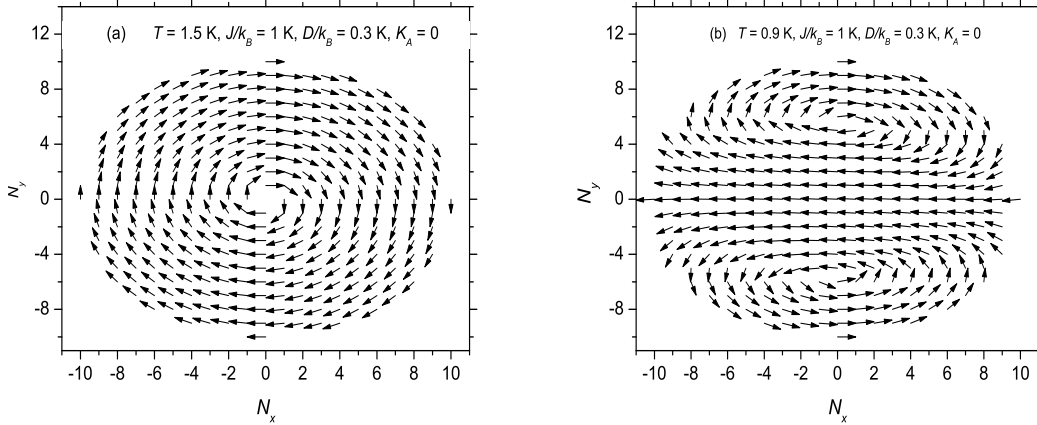


Figure 8. Calculated spontaneous spin configurations projected onto the xy -plane at (a) $T = 1.5$ K, and (b) $T = 0.9$ K, respectively. Other used parameters are $R = 10a$, $\mathcal{J}/k_B = 1$ K, $D/k_B = 0.3$ K, and $K_A = 0$ K.

Therefore, as DM interaction increases, the single vortex structure becomes unstable, and magnetic domains will appear. It was found in experiments that magnetic skyrmions could be induced by external magnetic field [3, 4, 6, 15], which means that the applied field is able to stabilize the eddy structure. To test this idea, an external magnetic field of 0.1 tesla was

considered to be applied in the z -direction to do simulations for the nanodisk. Consequently, under the interaction of the applied field, $\langle S_z \rangle$ is rotated to the field direction, becoming positive in the whole temperature region, both $\langle S_z \rangle$ and $\langle S_y \rangle$ are well symmetric about the T -axis, all of them decay monotonously with arising temperature as shown in Figure 9(a). These magnetic behaviors indicate that a single magnetic structure has been generated on the disk by the applied magnetic field. Indeed, as depicted in Figure 9(b), we find now under the interaction of the external magnetic field a single magnetic vortex that occupies the whole disk in the temperature range when $\langle S_z \rangle$ is appreciable.

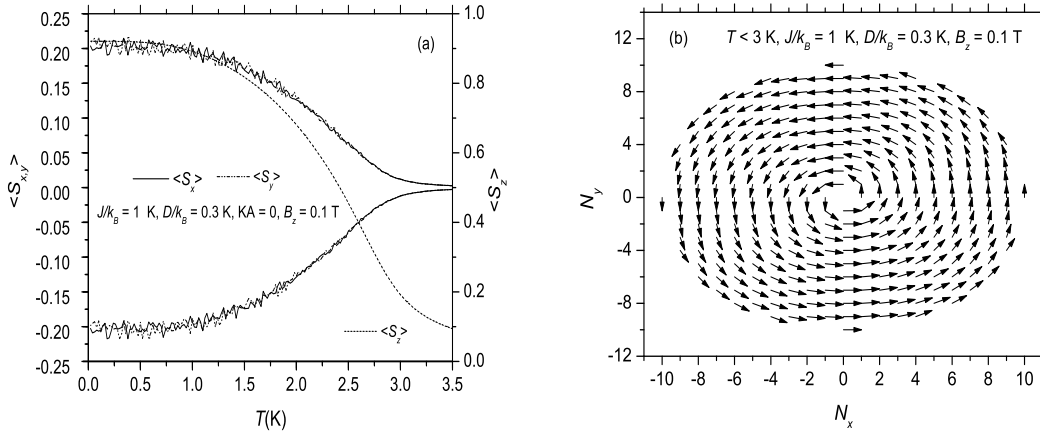


Figure 9. Calculated (a) $\langle S_x \rangle$, $\langle S_y \rangle$ and $\langle S_z \rangle$, (b) the spin configuration for the monolayer nanodisk in a magnetic field of 0.1 T applied along the z axis. Other parameters are $R = 10a$, $\mathcal{J}/k_B = 1$ K, $D/k_B = 0.3$ K, and $K_A = 0$ K, respectively.

F. Effects of Disk Size and External Magnetic Field

To further study the size effects, we then considered a larger monolayer nanodisk with $R = 30a$, $\mathcal{J}/k_B = 1$ K, $D/k_B = 0.1$ K, and $K_A = 0$, respectively, and did simulations by assuming that no external magnetic was present firstly. In this case, $\zeta = 10 < R$, so more magnetic structures will be self-organized on the disk plane. Though $\langle S_z \rangle$ and $\langle S_y \rangle$ decay monotonously with increasing temperature, the presence of the both $\langle S_z \rangle \leq 0$ and especially the asymmetry of $\langle S_x \rangle$ and $\langle S_y \rangle$, as shown in Figure 10, are the signs of existence of more than one structures on the disk plane. Indeed, as shown in Figure 11, two magnetic vortices

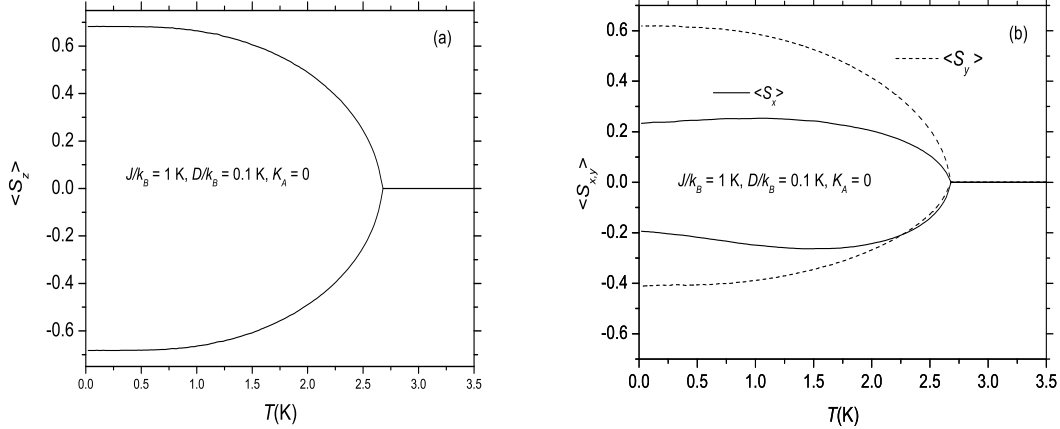


Figure 10. Calculated spontaneous (a) $\langle S_z \rangle$, (b) $\langle S_x \rangle$ and $\langle S_y \rangle$ for a larger monolayer nanodisk with $R = 30a$. Other parameters are $D/k_B = 0.1\text{ K}$, $J/k_B = 1\text{ K}$, and $K_A = 0$.

are generated in our simulation, they are separated by a magnetic strip. The two vortex centers are rotated as temperature changes, their distance is about $33a$, which is about three times of ζ , since three structures, one strip and two vortices, are formed between the centers. The square lattice cell is four-fold rotationally symmetric about the z -axis, but the asymmetric DM interaction has reduced the symmetry to two-fold, then only two vortices can be observed on the disk plane, we guess.

Once again, when an external magnetic field of 0.2 Tesla was considered to be applied in the z -direction to perform simulations, the two vortices and the strip between them shown in Figure 11 were merged to a single vortex around the center of the round disk as depicted in Figure 12. The ring structures there means that within the blank area the spins have all been polarized completely by the applied magnetic field to the z -direction. The Heisenberg and DM interactions compete with the external magnetic field, and they becomes stronger with decreasing temperature, so that the width of the ring grows and the blank area shrinks as T goes down.

Now we define a new quantity as $\langle A_{xy} \rangle = \sqrt{\langle S_x \rangle^2 + \langle S_y \rangle^2}$, here the average is made over all spins of a circle with radius r around the center. $\langle A_{xy} \rangle$ was calculated at different temperatures for the circles of different radii, three of them are now displayed in Figure 13(a). As temperature decreases, $\langle A_{xy} \rangle$ gets larger, and the ring width increases. Moreover, at every temperature, $\langle A_{xy} \rangle$ has a maximum near the edge, then fades quickly with decreasing $|r|$.

However, compared to the large magnitude of $\langle S_z \rangle$ as shown in Figure 13(b), the vortices are actually very weak.

G. Computational Efficiency

As described previously, our simulation approach is based on the principle of the lowest (free) energy, so that a code implemented with the algorithm is able to minimize the total (free) energy of the studied system automatically, and quickly converges to the equilibrium state. To test this hypothesis, both the total energies and total free energies of the small nanodisk with radius $R = 10a$ were recorded during computation at ten temperatures below 2.8 K as $B_z = 0$, and below 3.8 K when $B_z = -0.1$ K, respectively. Consequently, they were all found to decrease spontaneously and very quickly toward the equilibrium states during simulations, so that the computational speed has been greatly accelerated. For instance, in the absence of external magnetic field, as $\tau_0 = 10^{-5}$, $\Delta T = -0.02$ K, and other parameters assigned to the values given below Figure 1, it only took a few iterations to converge at very low temperatures, and less than 27 seconds to complete the whole simulation below the transition temperature T_M . Moreover, as an external magnetic field was assumed to be applied antiparallel to z -axis, the code converged very much faster. The reason might be that an external magnetic field is able to effectively suppress the energy barriers, so that the computational code takes much less time to tunnel through the smoothen energy barriers.

IV. CONCLUSIONS AND DISCUSSION

Based on our calculated results presented above, we can conclude: (a) The chirality of the single magnetic vortex on the nanodisk with the co-existence of DM and uniaxial anisotropic interactions is solely determined by the sign of D : the chirality is right-handed as $D > 0$, but left-handed as $D < 0$; (b) the external magnetic field applied perpendicular to the z -axis can not change the chirality of the magnetic vortice, it can only enhance the magnetizations in the field direction, and increase the transition temperature so that the vortex structure persists to higher temperatures as observed in experiments [4]; (c) Increasing the disk size or DM interaction strength gives rise to formation of magnetic domains, such as magnetic strips and vortices, on the disk plane, however applying external magnetic field normal to

the disk plane is able to stabilize the vortex structure and induce skyrmions [4].

We stress finally that in our SCA model the spins in the Hamiltonian are treated as quantum operators, and all physical quantities have been evaluated with quantum theory. From our simulations done so far it can be found that the computational speed has been considerably accelerated by this new computational approach, and the final simulated results are all reasonable physically [17–20], especially some of them are well consistent with experiment [20]. Therefore, we believe that the new approach can be applied to other sophisticated magnetic systems where various complicated interactions exist.

Acknowledgements

Z.-S. Liu acknowledges the financial supports by National Natural Science Foundation of China under grant No. 11274177. H. Ian is supported by the FDCT of Macau under grant 013/2013/A1, University of Macau under grants MRG022/IH/2013/FST and MYRG2014-00052-FST, and National Natural Science Foundation of China under Grant No. 11404415.

-
- [1] I. E. Dzyaloshinsky, *J. Phys. Chem. Solids* 4, 241 (1958)
 - [2] T. Moriya, *Phys. Rev. Lett.* 4, 228 (1960).
 - [3] A. Tonomura, X. Yu, K. Yanagisawa, T. Matsuda, Y. Onose, N. Kanazawa, H. S. Park, and Y. Tokura, *Nano Lett.* 12, 1673 (2012).
 - [4] X. Z. Yu, N. Kanazawa, Y. Onose, K. Kimoto, W. Z. Zhang, S. Ishiwata, Y. Matsui, and Y. Tokura, *Nat. Mater.* 10, 106 (2011).
 - [5] H. Wilhelm, M. Baenitz, M. Schmidt, U. K. Röler, A. Leonov, and A.N. Bogdanov, *Phys. Rev. Lett.* 107, 127203 (2011).
 - [6] X. Z. Yu, Y. Onose, N. Kanazawa, J. H. Park, J. H. Han, Y. Matsui, N. Nagaosa, and Y. Tokura, *Nature* 465, 901 (2010).
 - [7] S. Mühlbauer, B. Binz, F. Jonietz, C. Pfleiderer, A. Rosch, A. Neubauer, R. Georgii, and P. Böni, *Science* 323, 915 (2009).
 - [8] Stefan Heinze, Kirsten Von Bergmann, Matthias Menzel, Jens Brede, André Kubetzka, Roland Wiesendanger, Gustav Bihlmayer, Stefan Blügel, *Nature Physics* 7 (9), 713 (2011).
 - [9] M. Bode, M. Heide, K. von Bergmann, P. Ferriani, S. Heinze, G. Bihlmayer, A. Kubetzka, O. Pietzsch, S. Blügel and R. Wiesendanger, *Nature* 447, 190 (2007)

- [10] T. H. R. Skyrme, Nucl. Phys. 31, 556 (1962).
- [11] A. Wachowiak, J. Wiebe, M. Bode, O. Pietzsch, M. Morgenstern, and R. Wiesendanger, Science 298, 577 (2002)
- [12] T. Shinjo, T. Okuno, R. Hassdorf, K. Shigeto, and T. Ono, Science 389, 930 (2000)
- [13] S. B. Choe, Y. Acremann, A. Scholl, A. Bauer, A. Doran, J. Stöhr, and H. A. Padmore, Science 304, 420 (2004).
- [14] M. Y. Im, P. Fischer, K. Yamada, T. Sato, Y. Nakatani, and T. Ono, Nat. Commun. 3, 983 (2012).
- [15] W. Münzer, A. Neubauer, T. Adams, S. Mühlbauer, C. Franz, F. Jonietz, R. Georgii, P. Böni, B. Pedersen, M. Schmidt, A. Rosch, and C. Pfleiderer, Phys. Rev. B 81, 041203 (2010).
- [16] N. S. Kiselev, A. N. Bogdanov, R. Schäfer, and U. K. Röβler, J. Phys. D: Appl. Phys. 44, 392001 (2011).
- [17] Z.-S. Liu, V. Sechovský, and M. Diviš, J. Phys.: Condens. Matter 23, 016002 (2011).
- [18] Z.-S. Liu, V. Sechovský, and M. Diviš, Physica E 59, 27 (2014).
- [19] Z.-S. Liu, V. Sechovský, and M. Diviš, Physica E 62, 123 (2014).
- [20] Z.-S. Liu, V. Sechovský, and M. Diviš, Phys. Status Solidi B 249, 202 (2012).
- [21] Y. M. Luo, C. Zhou, C. Won, and Y. Z. Wu, Effect of Dzyaloshinskii Moriya interaction on magnetic vortex, arXiv:1401.3292v1.
- [22] H. Y. Kwon, S. P. Kang, Y. Z. Wu and C. Won J. Appl. Phys. 80, 133911 (2013).

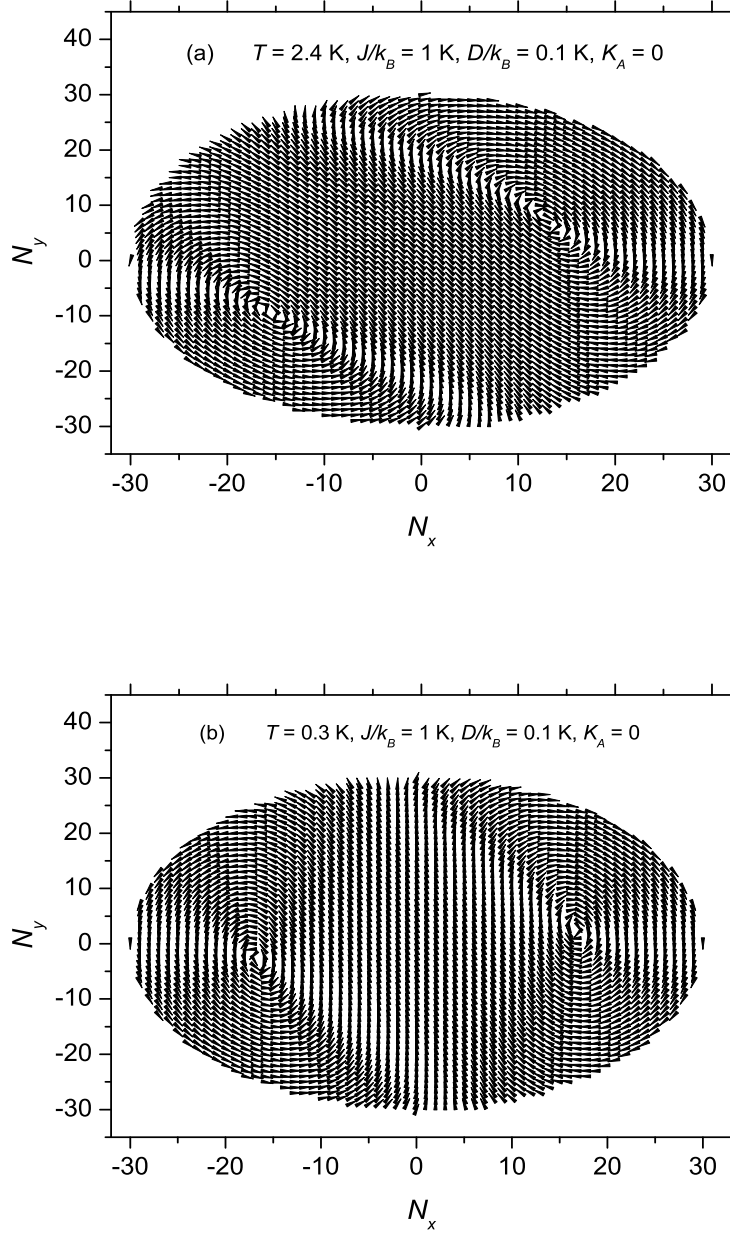


Figure 11. Calculated spontaneous spin configurations projected onto the xy -plane for the nanodisk with $R = 30a$ at (a) $T = 2.4 \text{ K}$, and (b) $T = 0.3 \text{ K}$, respectively. Other used parameters are $J/k_B = 1 \text{ K}$, $D/k_B = 0.1 \text{ K}$, and $K_A = 0$.

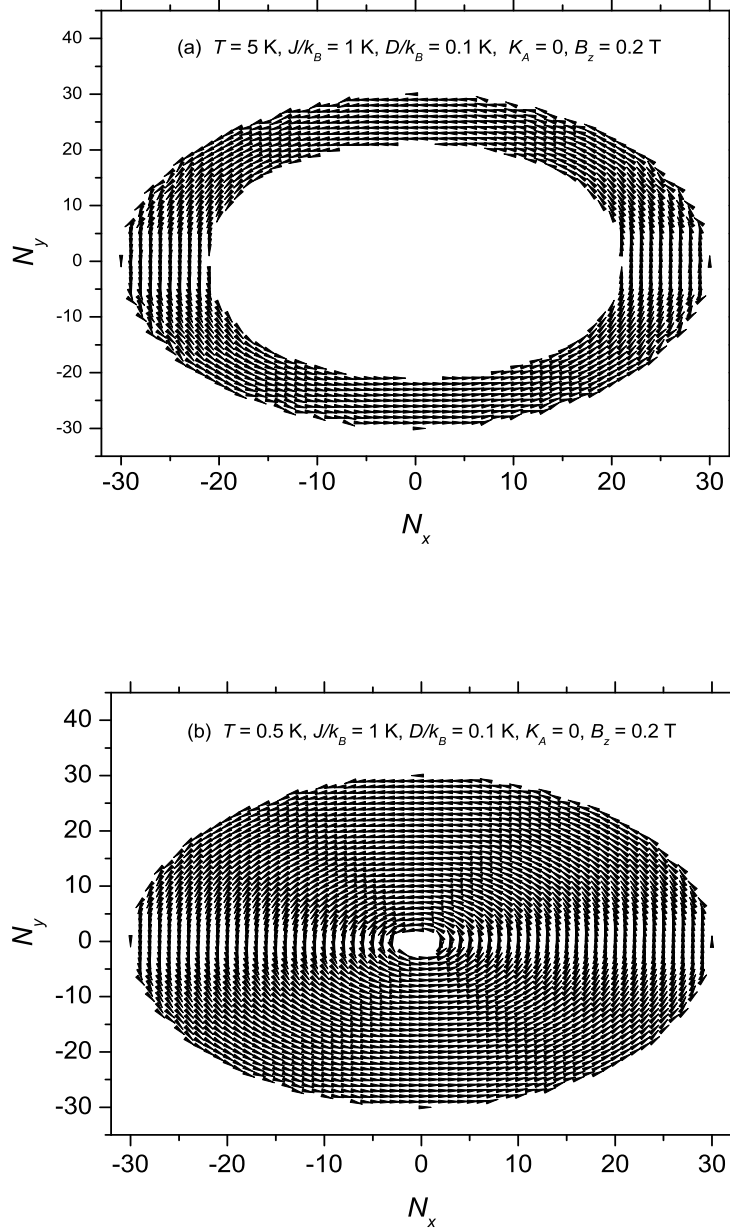


Figure 12. Calculated spin configurations projected onto the xy -plane for the nanodisk with $R = 30a$ within a magnetic field of 0.2 Tesla applied along the z -axis, at $T =$ (a) 5 K, and (b) 0.5 K, respectively. Other used parameters are $D/k_B = 0.1 \text{ K}$, $J/k_B = 1 \text{ K}$, and $K_A = 0 \text{ K}$.

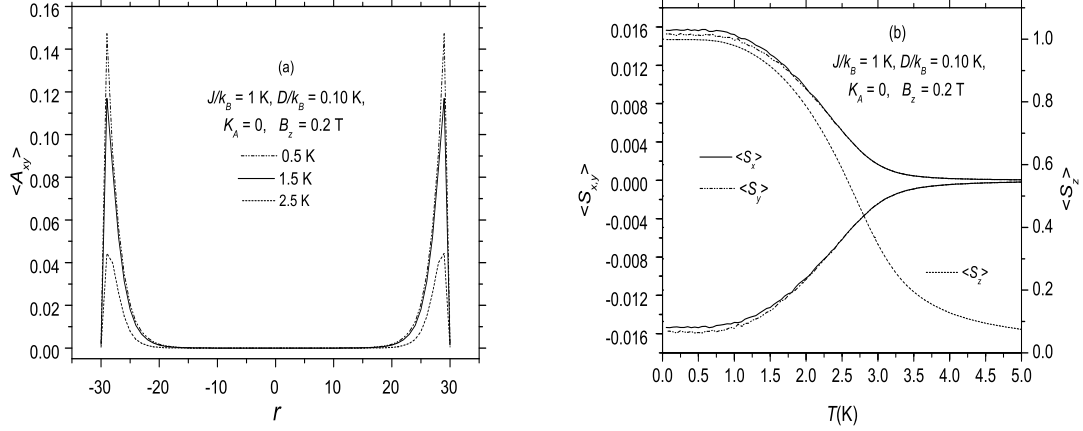


Figure 13. Calculated (a) $\langle A_{xy} \rangle$ at different temperatures as the functions of r , (b) $\langle S_x \rangle$, $\langle S_y \rangle$ and $\langle S_z \rangle$ as the functions of T , assumed in an magnetic field of 0.2 Tesla applied in the z direction for the nanodisk with $R = 30a$. Other used parameters are $\mathcal{J}/k_B = 1$ K, $D/k_B = 0.1$ K, and $K_A = 0$.